American Mineralogist, Volume 82, pages 143–148, 1997

Structure of synthetic $Li_2(Mg,Cu)Cu_2[Si_2O_6]_2$: A unique chain silicate related to pyroxene

HIROYUKI HORIUCHI,[1] AKIHIRO SAITO,[1] TOSHINAGA TACHI,[2] AND HIROSHI NAGASAWA[2]

[1]Mineralogical Institute, Faculty of Science, University of Tokyo, 7-3-1 Hongo, Bunkyo-ku, Tokyo 113, Japan
[2]Department of Chemistry, Faculty of Science, Gakushuin University, 1-5-1 Mejiro, Toshima-ku, Tokyo 171, Japan

ABSTRACT

A unique Cu-bearing chain silicate, $Li_2(Mg,Cu)Cu_2[Si_2O_6]_2$, was synthesized, and the structure was determined by single-crystal X-ray diffraction techniques. The structure was found to be triclinic, space group $P\bar{1}$, with unit-cell parameters a = 5.7068(7), b = 7.4784(9), c = 5.2193(3) Å, α = 99.911(8), β = 97.436(8), γ = 84.52(1)°, and Z = 1. The arrangement of zweier single chains, $[Si_2O_6]$, differs significantly from chain arrangements in the pyroxene and pyroxenoid structures, and the "I-beam" description of the pyroxene structure is not applicable. The structure may be classified as a new derivative type of the pyroxene structure, with an "oblique I-beam". Cu atoms are coordinated by four O atoms in a square-planar arrangement with 1.94–2.00 Å for Cu-O and two O atoms with longer Cu-O distances of 2.41–2.92 Å, consistent with the crystal-field stabilization of the d^9 electronic structure of Cu^{2+}. The square-planar CuO_4 units form a $[Cu_nO_{2n+2}]$ ribbon with n = 3 in the structure, which is also found in Cu-bearing chain silicates such as shattuckite and planchéite with $n > 3$. Mg is octahedrally coordinated by O atoms, but the configuration is affected by the partial replacement by Cu.

INTRODUCTION

Co- and Ni-bearing silicates have been studied mainly for the purpose of simulating the structural behavior of ferromagnesian silicate minerals under the high-temperature and high-pressure conditions prevailing in the Earth's interior. However, the crystal-chemical behavior of Cu-bearing silicates is different, possibly because of the electronic configuration of Cu^{2+}. Most of these naturally occurring minerals are hydrous or hydrated silicates and some are chain silicates. The following are examples of Cu-bearing silicate minerals that have chain structures: shattuckite, $Cu_5[Si_2O_6]_2(OH)_2$ (Mrose and Vlisidis 1966; Kawahara 1976; Evans and Mrose 1966, 1977); planchéite, $Cu_8[Si_4O_{11}]_2(OH)_4{\cdot}xH_2O$ (Evans and Mrose 1966, 1977); and liebauite, $Ca_6Cu_{10}[Si_{18}O_{52}]$ (Zöller et al. 1992). Liebauite is one of the few anhydrous Cu-bearing minerals. The layer silicate cuprorivaite, $CaCu[Si_4O_{10}]$ (Mazzi and Pabst 1962), is another example of a natural anhydrous Cu-bearing phase. On the other hand, most synthetic Cu-bearing chain silicates are anhydrous. Typical examples include $Na_2Cu_3[Si_4O_{12}]$ (Kawamura and Kawahara 1976), $Na_4Cu_2[Si_8O_{20}]$ (Kawamura and Kawahara 1977), $CuMg[Si_2O_6]$ (Breuer et al. 1986), and $CaBa_3Cu[Si_6O_{17}]$ (Angel et al. 1990). However, synthetic Cu-bearing chain silicates related to pyroxene are rare in comparison with silicates containing Co, Ni, or Zn (e.g., Morimoto et al. 1970, 1974, 1975). Nevertheless, knowledge of the phase stabilities and Cu configurations of Cu-bearing silicate structures is important for understanding the mineralogy and geochemistry of transition metals.

Examples of Cu-bearing silicates with single-chain structures are also quite rare. The mineral shattuckite and synthetic $CuMg[Si_2O_6]$ and $Na_2Cu_3[Si_4O_{12}]$ are the only known examples. $CuMg[Si_2O_6]$ was reported to be analogous to the clinopyroxene structure with space group $P2_1/c$, with an ordered arrangement of Mg and Cu as determined by the semiquantitative comparison of observed and calculated X-ray powder diffraction intensities (Breuer et al. 1986). However, the detailed structure is unknown. The configuration of the $[Si_2O_6]$ chain of shattuckite is similar to that of pyroxene with straight chains, but the cation arrangement is different from that of pyroxene. The structure of planchéite is a derivative structure of shattuckite but with amphibole-type double chains instead of single chains. The $[Si_2O_6]$ unit of $Na_2Cu_3[Si_4O_{12}]$ is a single chain; however, it is different from that of pyroxene but similar to that of haradaite (Takéuchi and Joswig 1967).

Thus, Cu-bearing pyroxene or pyroxene-derivative structures are very rare, even though the ionic radius of Cu^{2+} is similar to that of other transition metal ions. In the present paper, a new Cu-bearing silicate structure with straight single chains is described and the crystal-chemical behavior of Cu^{2+} in the structure is discussed.

EXPERIMENTAL METHOD

Sample preparation and chemical analysis

The crystalline phase of $Li_2(Mg,Cu)Cu_2[Si_2O_6]_2$ was synthesized in an oxide-flux mixture, which was primarily prepared for the synthesis of Cu-bearing pyroxene.

0003–004X/97/0102–0143$05.00

TABLE 1. Results of chemical and structure analyses

Components	Chemical analysis		Result of structure analysis	
	wt% (expt.)	mole ratio	wt% (calc.)	mole ratio
SiO_2	50.6(4)	4	50.63	4
MgO	8.4(3)	0.99	7.39(3)	0.871(3)
CuO	33.7(4)	2.01	35.69	2.129
Li_2O	7.3(7)	1.16	6.3(1)	0.98(2)
Total	100		100	

Note: The weight percent values were normalized to a total of 100%, and the mole ratio values of SiO_2 were constrained to 4. The results of structure analysis were obtained by the refinement of site occupancies (see text) of Cu, M, and Li sites. Other sites were assumed to be fully occupied by each single atom.

TABLE 2. Crystallographic data and experimental conditions for structure analysis

Chemical formula	$Li_2(Mg,Cu)Cu_2[Si_2O_6]_2$, $Z = 1$
Space group	$P\bar{1}$
Calculated density	3.580 g/cm³
Size of specimen	0.10 × 0.20 × 0.37 mm³
X-ray source	Mo$K\alpha$ 40kV, 25mA (fine focus)
Monochromator	Pyrolytic graphite
Apparatus	AFC5S/Rigaku
Scan mode, width, and speed	2θ ω, $\Delta 2\theta = 1.4°(\tan\theta) + 0.65°$, 6.0°/min
Obs. refl.	4526 ($F_{obs} \neq 0$), $0° < 2\theta \leq 100°$ (hemisphere)
Indep. refl.	4221 ($F_{obs} \neq 0$), $R_w = 0.041$, $R = 0.057$
Refl. used	3573 ($F_{obs} \geq 5\sigma_{Fobs}$), $R_w = 0.041$, $R = 0.047$

The molar ratio of oxides was $MgO:CuO:SiO_2 = 1:1:2$, and that of the flux was $Li_2O:MoO_3:V_2O_5 = 42.8:51.2:6.0$. The percentage of MgO-CuO-SiO_2 mixture was about 20% of the total weight of the sample. The mixture was heated to 850 °C for 3 h in a platinum crucible. The temperature was gradually decreased from 850 to 650 °C over 8 d, after which the mixture was slowly cooled to room temperature by turning off the electricity. All processes were performed in air. In the high-temperature reaction, Li_2O, MoO_3, and V_2O_5 serve as the flux, although Li is incorporated into the final product. Transparent greenish blue crystals (1–2 mm) were obtained by dissolving surrounding materials in warm dilute HCl.

The chemical composition of the products was analyzed by electron probe microanalysis for Mg, Cu, and Si, and by ICP for Li. The results are shown in Table 1 together with the chemical composition obtained from structure analysis, which is discussed later. On the basis of the chemical analysis, the idealized chemical formula is assumed to be $Li_2MgCu_2Si_4O_{12}$.

Structure determination and refinement

The crystal-structure determination was performed using single-crystal X-ray diffraction techniques. The crystals are often twinned, so the single-crystal specimen for the structure determination was obtained by careful separation from the twinned crystal. Experimental conditions for X-ray diffraction data collection and reliability factors for the final results of the refinement are given in Table 2. The structure analysis was performed using 3573 independent reflections with $F_{obs} \geq 5\sigma_{Fobs}$. An absorption correction was made by using a calibration curve obtained by the ψ scan method. Lattice parameters were determined by the least-squares method using 22 reflections in the range 50–60° 2θ measured by a four-circle single-crystal diffractometer. The choice of the unit cell follows the rules of Donnay (1943). Refined values are $a = 5.7068(7)$, $b = 7.4784(9)$, $c = 5.2193(3)$ Å, $\alpha = 99.911(8)$, $\beta = 97.436(8)$, $\gamma = 84.52(1)°$, and $V = 216.96$ Å³. Table 3 gives refined atomic coordinates and atomic displacement factors.

The positions of Mg, Cu, Si, and O were first determined using a combination of Patterson, Fourier, and difference-Fourier maps. As a result, four independent atomic positions were found for cations and six for O atoms. They were initially assigned as Mg, Cu, Si1, and Si2 for cations and as O1–O6 for the O atoms. The value of $1/\sigma^2_{Fobs}$ was used as a weight for each reflection. The weighted residual $R_w = 0.068$ was obtained after the least-squares refinement of the atomic positions and anisotropic displacement factors. The site occupancies were assumed to be 100% for the above atoms.

Further difference-Fourier syntheses using the above refined atomic coordinates revealed positive residual peaks at the position (M) in which Mg was assigned, and at another new position (P). No other significant residual peaks were observed. From the chemical composition, the M position was modeled as a statistical distribution of Mg and Cu with a total occupancy of unity. The value of 0.871(3) was obtained for the occupancy factor of Mg in the M site by least-squares refinement. As a result, the statistical distribution of M is 0.87Mg + 0.13Cu. The P site was assigned to Li on the basis of the chemical composition and the electron density on the Fourier and difference-Fourier maps. The occupancy value of the Li site refined to 0.98(2). Therefore, the Li site was assumed to be fully occupied within experimental error. Finally, difference-Fourier syntheses using all atoms, including the statistical distribution of Mg and Cu for M, were calculated and no residual peaks were observed. Although the space group was initially assumed to be $P1$, the structure model finally refined to the space group $P\bar{1}$. This result is consistent with the crystal structure and morphology.

According to the classification by Liebau (1985), the actual structure formula was concluded to be $Li_2^{[3]}(Mg_{0.87},Cu_{0.13})^{[6O]}Cu_2^{[4i]}\{uB,1\frac{1}{\infty}\}[^2Si_2O_6]_2$. From the structure formula, the chemical composition was calculated as shown in Table 1. These values are slightly different from the results of the chemical analysis obtained by EPMA and ICP, in particular for Cu, possibly because EPMA analyzed only Mg, Si, and Cu, and Li was analyzed separately by ICP. Table 4 contains F_o and F_c values for the final results.[1] Interatomic distances and angles are given

[1] A copy of Table 4 may be ordered as Document AM-97-632 from the Business Office, Mineralogical Society of America, 1015 Eighteenth Street NW, Suite 601, Washington, DC 20036. Please remit $5.00 in advance for the microfiche.

TABLE 3. Refined atomic coordinates and atomic displacement factors

Atom	x	y	z	B_{eq} (Å²)	β_{11}	β_{22}	β_{33}	β_{12}	β_{13}	β_{23}
M	0	0	0	0.43	3.8(3)	1.8(2)	4.3(4)	−0.6(2)	2.3(3)	−0.5(2)
Cu	0.83770(6)	0.18327(5)	0.50890(8)	0.44	3.37(8)	1.88(4)	4.8(1)	−0.04(4)	1.81(7)	0.09(5)
Si1	0.4093(1)	0.1859(1)	0.7795(2)	0.33	1.7(2)	1.9(1)	3.5(2)	0.0(1)	0.9(2)	0.2(1)
Si2	0.2224(1)	0.3721(1)	0.3003(2)	0.30	1.7(2)	1.6(1)	3.1(2)	0.1(1)	0.4(2)	0.1(1)
Li	0.760(1)	0.409(1)	0.073(2)	1.94	5(2)	13(1)	25(3)	0(1)	−2(2)	10(2)
O1	0.6745(3)	0.0955(3)	0.7625(4)	0.62	2.3(4)	4.1(3)	6.9(6)	0.9(3)	1.8(4)	1.5(4)
O2	0.4109(3)	0.3111(3)	0.0762(4)	0.53	2.9(4)	3.4(3)	4.4(6)	−0.5(3)	1.9(4)	−0.8(3)
O3	0.3602(3)	0.3430(3)	0.5862(4)	0.57	4.2(4)	3.2(3)	4.9(6)	−0.8(3)	−1.0(4)	1.9(3)
O4	0.1953(3)	0.0543(3)	0.7306(4)	0.51	3.2(4)	2.4(3)	5.7(6)	−1.1(3)	1.2(4)	−0.3(3)
O5	0.1354(4)	0.5789(3)	0.2764(4)	0.63	5.8(5)	1.8(3)	6.9(6)	0.4(3)	0.7(5)	0.2(3)
O6	−0.0014(3)	0.2467(3)	0.2285(4)	0.45	2.8(4)	2.3(3)	4.8(6)	−0.5(3)	1.1(4)	0.1(3)

Note: M = 0.87Mg + 0.13Cu. Anisotropic atomic displacement factors are shown as × 10^3. Equivalent isotropic atomic displacement factors: $B_{eq} = \frac{4}{3}\Sigma_{ij}(\beta_{ij}a_ia_j)$. Estimated standard errors refer to the last digits. Coefficients of β_{ij} are given as $\exp[-(\beta_{11}h^2 + \beta_{22}k^2 + \beta_{33}l^2 + 2\beta_{12}hk + 2\beta_{13}hl + 2\beta_{23}kl)]$.

in Table 5. The program RFINE II (Finger 1969) was used for the structure-refinement calculations.

DESCRIPTION OF THE STRUCTURE

The crystal structure projected along the *c* axis is illustrated in Figure 1. Single $[Si_2O_6]$ chains are aligned along the *c* axis. The bands of tetrahedral groups that are constructed of $[Si_2O_6]$ chains and other cation polyhedral bands that are composed of Mg, Cu, and Li atoms are alternately layered parallel to (110). The SiO_4 tetrahedra that form $[Si_2O_6]$ chains are quite regular in configuration, as are those observed in most pyroxenes. Their Si-O distances are in the range 1.600–1.668 Å. The distances from Si to the bridging O atoms in $[Si_2O_6]$ chains, 1.633–1.668 Å, are larger than other Si-O distances, 1.600–1.623 Å, because of Si-Si repulsion.

The M site, which contains 0.87Mg + 0.13Cu, is octahedrally coordinated by six O atoms [4 + 2]. The M-O distances are in the range 2.017–2.225 Å. However, it seems that the partial replacement of Mg by Cu in the MO_6 octahedra affects its coordination and results in square-planar distortion. The M-O4 and M-O6 distances are in the range 2.017–2.018 Å, which is shorter than the two M-O1 distances of 2.225 Å.

CuO_6 is greatly distorted from octahedral configuration and forms a square-planar coordination. The distances from Cu to two O atoms are 2.415 and 2.918 Å. These distances are much greater than the distances from Cu to the other four O atoms, which are in the range 1.940–1.998 Å.

The Li site is displaced from the center of the coordination polyhedra. As a result, Li and three O atoms form a deformed trigonal pyramid, LiO_3. The Li-O distances are in the range 1.928–2.193 Å. The distances from Li to O atoms that do not belong to the LiO_3 pyramid are longer than 2.431 Å.

DISCUSSION

The structural characteristics of the layered arrangement of tetrahedral and octahedral bands are similar to those of pyroxene. One of the most remarkable differences between the crystal structure of $Li_2(Mg,Cu)Cu_2[Si_2O_6]_2$ and those of the pyroxene group is that the bands of tetrahedral groups are shifted with respect to each other along [$\bar{1}$10]. As a result, the "I-beam" description (Cameron and Papike 1981), which is commonly used to characterize pyroxene structures, is not applicable to this structure. However, the I-beam is deformed as an oblique I-beam, shown as shaded regions in Figure 1.

The structure of $Li_2(Mg,Cu)Cu_2[Si_2O_6]_2$ is compared with related structures in Figure 2, using the same systematics as those reported by Takéuchi and Koto (1977). From the oblique I-beam presentation, the projected structure of Figure 2b is apparently similar to those of pyroxenoids (Fig. 3c) such as bustamite, $Ca_3Mn_3[Si_3O_9]_2$; pectolite, $NaCa_2[Si_3O_8(OH)]$; wollastonite, $Ca_3[Si_3O_9]$; etc. (Peacor and Prewitt 1962; Prewitt and Buerger 1963; Takéuchi and Koto 1977). However, the form of the se-

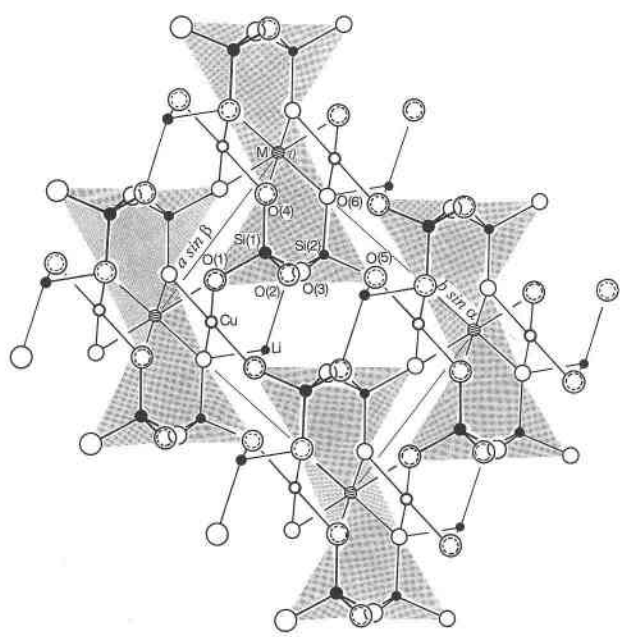

FIGURE 1. Crystal structure of $Li_2(Mg, Cu)Cu_2[Si_2O_6]_2$ projected along the *c* axis. Large solid circles = Si, large open circles = O, hatched circles = M (Mg,Cu), small open circles = Cu, small solid circles = Li. The oblique I-beam parts are shaded. Interatomic distances <2.4 Å are shown by solid lines.

TABLE 5. Interatomic distances (Å) and angles (°) of $Li_2(mg,Cu)Cu_2[Si_2O_6]_2$

M-O distances		Cu-O distances	
M-O1[a]	2.225(3) × 2	Cu-O1	1.945(3)*
M-O4[b]	2.018(4) × 2	Cu-O3	2.917(3)
M-O6	2.017(2) × 2	Cu-O4[h]	2.415(2)
Mean[4]	2.018	Cu-O4[e]	1.998(2)*
		Cu-O5[f]	1.940(2)*
		Cu-O6	1.970(3)*
		Mean[4]	1.963
O-M-O angles		**O-Cu-O angles**	
O1[b]-M-O4[b]	89.1(1) × 2	O1-Cu-O4[h]	85.6(1)
O1[b]-M-O4[c]	90.9(1) × 2	O1-Cu-O4[e]	90.0(1)*
O1[b]-M-O6	89.3(1) × 2	O1-Cu-O5[f]	92.5(1)*
O1[b]-M-O6[d]	90.8(1) × 2	O1-Cu-O6[h]	173.9(1)*
O1[b]-M-O1[e]	180	O4[c]-Cu-O4[e]	89.3(1)
O4[a]-M-O6	97.8(1) × 2	O4[c]-Cu-O5[f]	93.2(1)
O4[a]-M-O6[d]	82.2(1) × 2	O4[c]-Cu-O6[h]	94.3(1)
O4[a]-M-O4[c]	180	O4[e]-Cu-O5[f]	176.6(1)*
O6-M-O6[d]	180	O4[e]-Cu-O6[h]	83.9(1)*
		O5[f]-Cu-O6[h]	93.6(1)*
Si1-O distances		**Si2-O distances**	
Si1-O1	1.605(2)	Si2-O2	1.668(3)
Si1-O2[g]	1.665(3)	Si2-O3	1.633(3)
Si1-O3	1.658(3)	Si2-O5	1.600(2)
Si1-O4	1.609(2)	Si2-O6	1.623(2)
Mean	1.634	Mean	1.631
O-Si1-O angles		**O-Si2-O angles**	
O1-Si1-O2[g]	105.9(1)	O3-Si2-O2	108.7(1)
O1-Si1-O3	108.5(2)	O3-Si2-O5	114.4(1)
O1-Si1-O4	118.5(1)	O3-Si2-O6	109.7(2)
O2[g]-Si1-O3	102.2(1)	O2-Si2-O5	104.5(2)
O2[g]-Si1-O4	109.4(2)	O2-Si2-O6	109.6(1)
O3-Si1-O4	111.0(1)	O5-Si2-O6	109.8(1)
Li-O distances		**O-Li-O angles**	
Li-O1[b]	2.66(1)	O2-Li-O2[i]	92.5(4)
Li-O2	2.19(1)**	O2-Li-O3[f]	85.6(4)
Li-O2[i]	2.43(1)	O2-Li-O5[i]	117.6(6)**
Li-O3[f]	2.45(1)	O2-Li-O6[h]	108.7(6)**
Li-O5[h]	2.60(1)	O2[i]-Li-O3[f]	64.0(3)
Li-O5[i]	2.01(2)**	O2[i]-Li-O5[i]	70.4(5)
Li-O6[h]	1.93(1)**	O2[i]-Li-O6[h]	157.5(5)
Mean[3]	2.04	O3[f]-Li-O5[i]	129.5(6)
		O3[f]-Li-O6[h]	109.2(7)
		O5[i]-Li-O6[h]	104.5(5)**

Note: Cation-O distances <2.7 Å and angles associated with cation-O distances <2.6 Å are listed. Mean[4] is the mean distance for square-planar coordination for M and Cu, and mean[3] is the value for three shorter Li-O bonds. M = 0.87Mg + 0.13Cu. Symmetry operation codes: none = x, y, z; a = $-1 + x, y, 1 + z$; b = $x, y, -1 + z$; c = $x, -y, 1 - z$; d = $-x, -y, -z$; e = $1 - x, -y, 1 - z$; f = $1 - x, 1 - y, 1 - z$; g = $x, y, 1 + z$; h = $1 - x, 1 - y, -z$; i = $1 + x, y, z$.

* Square-planar O atoms with Cu.

** O atoms pyramidally coordinated to Li.

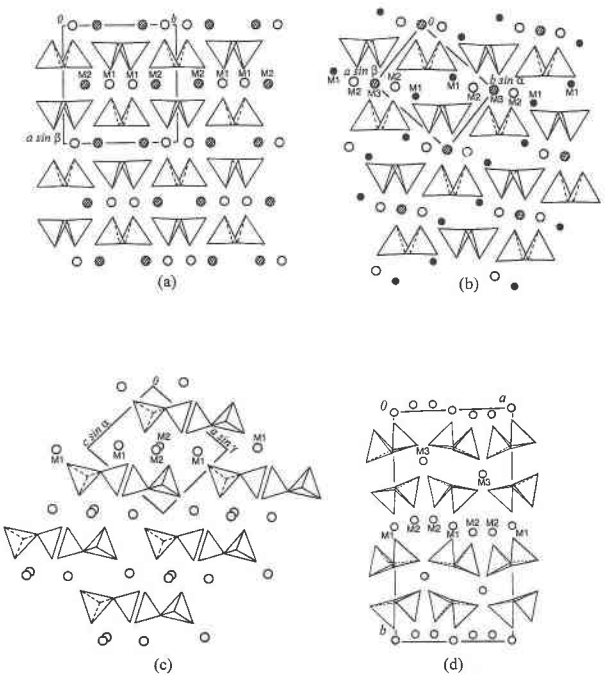

FIGURE 2. Comparison of the structures of (**a**) pyroxene, M1M2$[Si_2O_6]$; (**b**) $Li_2(Mg,Cu)Cu_2[Si_2O_6]_2$, where M1 = Li, M2 = Cu, and M3 = (Mg,Cu); (**c**) wollastonite, $Ca_3[Si_3O_6]$, where M1 = M2 = M3 = Ca; and (**d**) shattuckite, $Cu_5[Si_2O_6]_2(OH)_2$, where M1 = M2 = M3 = Cu. The configurations of each $[Si_2O_6]$ chain of pyroxene, $Li_2(Mg,Cu)Cu_2[Si_2O_6]_2$, and shattuckite resemble each other, but the arrangement of the chains is different.

quence of SiO_4 tetrahedra along the c axis of $Li_2(Mg,Cu)Cu_2[Si_2O_6]_2$ is different from the pyroxenoid structure but is very similar to the pyroxene structure (Fig. 2a). Furthermore, the arrangement of cations in the polyhedral bands is different from those of both pyroxene and pyroxenoid structures. In pyroxene, the arrangement of pairs of cations such as M1-M1-M2-M2-M1-M1-M2-M2 is observed in the polyhedral bands projected along the $[Si_2O_6]$ chain, where, for example, M1 and M2 are occupied by atoms such as Ca and Mg, respectively. However, in $Li_2(Mg,Cu)Cu_2[Si_2O_6]_2$, an additional cation, M3, intrudes into the polyhedral bands, resulting in M1-M1-M2-M3-M2-M1-M1-M2-M3-M2 as an ideal arrangement, where M1 is Li, M2 is Cu, and M3 is the atom site with the statistical distribution of 0.87Mg and 0.13Cu, respectively. The Li atoms are greatly displaced from the center of the polyhedra. From the view point of the arrangement of $[Si_2O_6]$ chains, the structure of shattuckite (Fig. 2d) (Kawahara 1976; Evans and Mrose 1977) is also of the oblique I-beam type. As a result, two types of polyhedral bands, sandwiched by tetrahedral bands, are observed in the shattuckite structure. One has the arrangement M1-M1-M2-M2, whereas the other contains only M3, where M1, M2, and M3 all contain Cu.

The square-planar CuO_4 configuration observed in the structure of $Li_2(Mg,Cu)Cu_2[Si_2O_6]_2$ is commonly found in crystal structures that contain Cu^{2+}, such as tenorite, CuO (Bragg et al. 1965), and other Cu-bearing chain silicates. If we assume that the M3 site is occupied by Cu in the $Li_2(Mg,Cu)Cu_2[Si_2O_6]_2$ structure, CuO_4 square-planar units form finite ladderlike ribbons of $[Cu_nO_{2n+2}]$ with n = 3, as shown in Figure 3. The same ribbon is also observed in shattuckite (Kawahara 1976; Evans and Mrose 1977).

It is interesting that the ribbon with n = 6 is found in the structure of planchéite (Evans and Mrose 1977) and a ribbon with n = 2 is observed in the structure of synthetic $Na_2Cu_3[Si_4O_{12}]$ (Kawamura and Kawahara 1976).

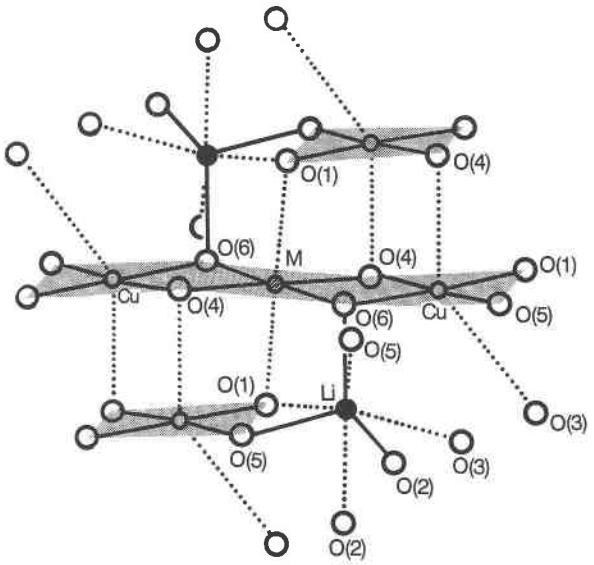

FIGURE 3. Schematic view along the direction nearly parallel to the Cu_3O_8 square-planar units in the structure of $Li_2(Mg,Cu)Cu_2[Si_2O_6]_2$. The shaded areas show a $[Cu_nO_{2n+2}]$ ribbon with $n = 3$.

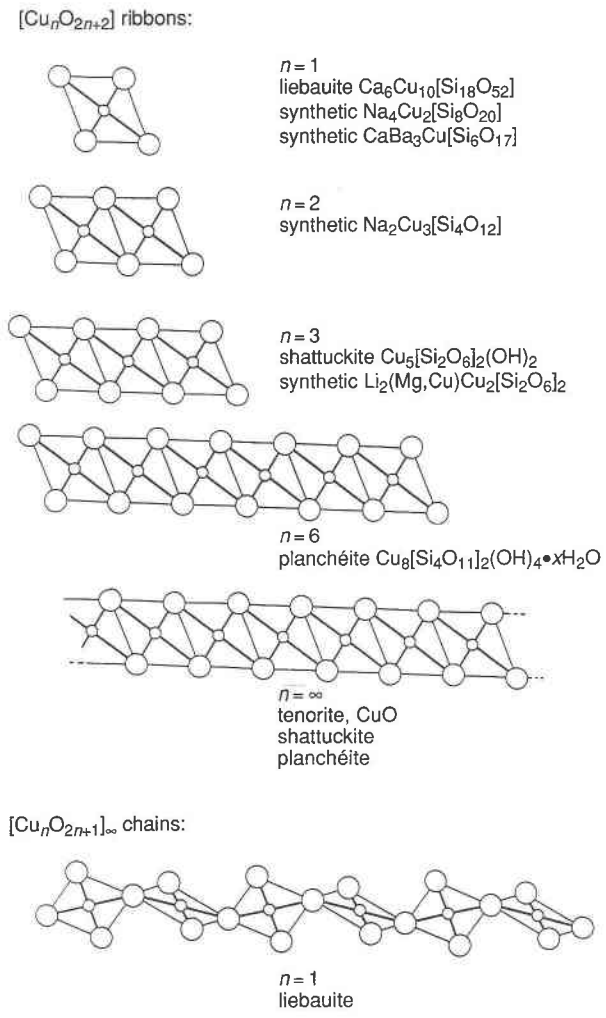

FIGURE 4. Classification of the Cu-O configuration in the structure of Cu-bearing chain silicates.

An infinite ribbon of $[Cu_nO_{2n+2}]$ with $n = \infty$, which is observed in tenorite, is also found in shattuckite and planchéite. In synthetic $Na_4Cu_2[Si_8O_{20}]$ (Kawamura and Kawahara 1977) and $CaBa_3Cu[Si_6O_{17}]$ (Angel et al. 1990), only isolated square-planar CuO_4 units are found. The ribbons of $[Cu_nO_{2n+2}]$ in silicate structures are not flat but generally folded. These ribbons of $[Cu_nO_{2n+2}]$ are sometimes bridged by sharing a corner O atom of another $[Cu_nO_{2n+2}]$ ribbon, making an infinite $[Cu_nO_{2n+1}]_\infty$ chain. The infinite $[Cu_nO_{2n+1}]_\infty$ chain with $n = 2$ in the $Na_2Cu_3[Si_4O_{12}]$ structure is an example, and in liebauite (Zöller et al. 1992) an infinite $[Cu_nO_{2n+1}]_\infty$ chain with $n = 1$ is observed in addition to an isolated square-planar CuO_4 unit. Thus, Cu-O configurations are classified into isolated square-planar CuO_4 units, ladderlike ribbons of $[Cu_nO_{2n+2}]$ with finite or infinite values of n, and an infinite $[Cu_nO_{2n+1}]$ chain with $n = \infty$ in Cu-bearing silicate structures. Cu-O configurations in Cu-bearing chain silicates are schematically classified in Figure 4.

In conclusion, the structure of $Li_2(Mg,Cu)Cu_2[Si_2O_6]_2$ is characterized as follows: (1) The spd^2 hybrid electronic configuration of Cu^{2+} strongly affects the O-atom arrangements around Cu, resulting in square-planar coordination; (2) strong Li-Li electrostatic repulsive forces result in a deformed LiO_3 trigonal pyramidal configuration; (3) owing to both the charge balance and the coordination of O atoms to Cu and Li, one extra cation intrudes into the cation polyhedral bands in comparison with pyroxene structures. Thus, the structure can be classified as a new derivative, "tpx," of the pyroxene group and is situated between pyroxene and other Cu-bearing chain silicate structures such as shattuckite and planchéite.

In the structures of synthetic $CaNi[Si_2O_6]$ and $CaCo[Si_2O_6]$ (Ghose et al. 1987), the O configurations surrounding transition elements such as Ni and Co have characteristics similar to those of the regular octahedra of pyroxene, although NiO_6 and CoO_6 octahedra are slightly deformed and thus show square-planar coordination. However, the deformation toward square-planar coordination is much less in comparison with CuO_6 in the structures of Cu-bearing chain silicates. Recently, the synthetic Cu-bearing orthopyroxene structure of $(Mg_{0.44},Cu_{0.56})Mg[Si_2O_6]_2$ was reported (Tachi et al. 1997, in preparation). The O-atom configuration surrounding (Mg,Cu) is not like the square-planar coordination of CuO_4 in $Li_2(Mg,Cu)Cu_2[Si_2O_6]_2$ but a distorted square-pyramidal coordination. Thus, the crystal-chemical behavior of Cu^{2+} in the chain silicate structure is greatly different from those of Mg^{2+}, Fe^{2+}, Co^{2+}, Ni^{2+}, etc., although the ionic radius of Cu^{2+} (0.73 Å; Shannon and Prewitt 1969) is within the range, 0.7–0.8 Å, of these cations. In conclusion, Cu-bearing pyroxene becomes stable only when Cu

is not a major component. On the other hand, if Cu is one of the main constituent elements, a finite ladderlike ribbon of $[Cu_nO_{2n+2}]$ is formed in the structure, and this affects the arrangement of the $[Si_2O_6]$ chain and leads to various unique chain structures.

Acknowledgments

The authors thank F. Liebau for his helpful discussion on the structures of Cu-bearing silicates and also for his careful review of our work, and R.C. Peterson and G. Giester for their critical readings of the manuscript. K. Sugiyama is thanked for his discussion on works related to Cu-bearing silicate minerals. H.H. was financially supported by Grant-in-Aid for Scientific Research B-07459008 of the Ministry of Education, the Japanese government, and by the Kazuchika Okura Memorial Foundation.

References cited

Angel, B.J., Ross, N.L., Finger, L.W., and Hazen, R.M. (1990) $Ba_3CaCuSi_6O_{17}$: A new {1B, 1½} [$^4Si_6O_{17}$] chain silicate. Acta Crystallographica, C46, 2028–2030.

Bragg, L., Claringbull, G.F., and Taylor, W.H. (1965) Crystal structures of minerals. In L. Bragg, Ed., The crystalline state, vol. IV, p. 94–95. Bell and Sons, London.

Breuer, K.-H., Eysel, W., and Behruzi, M. (1986) Copper(II) silicates and germanates with chain structures: II. Crystal chemistry. Zeitschrift für Kristallographie, 176, 219–232.

Cameron, M., and Papike, J.J. (1981) Structural and chemical variations in pyroxenes. American Mineralogist, 66, 1–50.

Donnay, J.D.H. (1943) Resetting a triclinic unit cell in the conventional orientation. American Mineralogist, 28, 507–511.

Evans, H.T., Jr., and Mrose, M.E. (1966) Shattuckite and planchéite: A crystal chemical study. Science, 154, 506–507.

——— (1977) The crystal chemistry of the hydrous copper silicates, shattuckite and planchéite. American Mineralogist, 62, 491–502.

Finger, L.W. (1969) Determination of cation distribution by least-squares refinement of single-crystal X-ray data. Carnegie Institution of Washington Yearbook, 67, 216–217.

Ghose, S., Wan, C., and Okamura, F.P. (1987) Crystal structures of $CaNiSi_2O_6$ and $CaCoSi_2O_6$ and some crystal-chemical relations in *C2/c* clinopyroxenes. American Mineralogist, 72, 375–381.

Kawahara, A. (1976) The crystal structure of shattuckite. Mineralogical Journal, 8, 193–199.

Kawamura, K., and Kawahara, A. (1976) The crystal structure of synthetic copper sodium silicate $Cu_3Na_2(Si_4O_{12})$. Acta Crystallographica, B32, 2419–2422.

——— (1977) The crystal structure of synthetic copper sodium silicate $CuNa_2(Si_4O_{10})$. Acta Crystallographica, B33, 1071–1075.

Liebau, F. (1985) Structural chemistry of silicates, 347 p. Springer-Verlag, Berlin.

Mazzi, F., and Pabst, A. (1962) Reexamination of cuprorivaite. American Mineralogist, 47, 409–411.

Morimoto, N., Akimoto, S., Koto, K., and Tokonami, M. (1970) Crystal structures of high pressure modifications of Mn_2GeO_4 and Co_2SiO_4. Physics of Earth and Planetary Interiors, 3, 161–165.

Morimoto, N., Tokonami, M., Watanabe, M., and Koto, K. (1974) Crystal structures of three polymorphs of Co_2SiO_4. American Mineralogist, 59, 475–485.

Morimoto, N., Nakajima, Y., Syono,Y., Akimoto, S., and Matsui, Y. (1975) Crystal structures of pyroxene-type $ZnSiO_3$ and $ZnMgSi_2O_6$. Acta Crystallographica, B31, 1041–1049.

Mrose, M.E., and Vlisidis, A.C. (1966) Proof of the formula of shattuckite, $Cu_5(SiO_3)_4(OH)_2$ (abs). American Mineralogist, 51, 266–267.

Peacor, D.R., and Prewitt, C.T. (1963) Comparison of the crystal structures of bustamite and wollastonite. American Mineralogist, 48, 588–596.

Prewitt, C.T., and Buerger, M.J. (1963) Comparison of the crystal structures of wollastonite and pectolite. Mineralogical Society of America Special Paper, 1, 293–302.

Shannon, R.D., and Prewitt, C.T. (1969) Effective ionic radii in oxides and fluorides. Acta Crystallographica, B25, 925–946.

Tachi, T., Horiuchi, H., and Nagasawa, H. (1997) Structure of Cu-bearing orthopyroxene and its implication to the partitioning behavior of Cu^{2+} and the transition metal ions in the igneous processes. Physics and Chemistry of Minerals, in press.

Takéuchi, Y., and Joswig, W. (1967) The structure of haradaite and a note on the Si-O bond lengths in silicates. Mineralogical Journal, 5, 98–123.

Takéuchi, Y., and Koto, K. (1977) A systematics of pyroxenoid structures. Mineralogical Journal, 8, 272–285.

Zöller, M.H., Tillmanns, E., and Hentshel, G. (1992) Liebauite, $Ca_3Cu_5Si_9O_{26}$: A new silicate mineral with 14er single chain. Zeitschrift für Kristallographie, 200, 115–126.

Manuscript received May 3, 1995
Manuscript accepted October 7, 1996